ARTICLE

Enhanced Electric Double Layer Capacitance of Graphite Oxide Intercalated by Poly(sodium 4-styrensulfonate) with High Cycle Stability

Hae-Kyung Jeong,[†] Meihua Jin,[†] Eun Ju Ra,[†] Kyeu Yoon Sheem,[‡] Gang Hee Han,[†] Sivaram Arepalli,[†] and Young Hee Lee[†,*]

[†]BK21 Physics Division, Department of Energy Science, Center for Nanotubes and Nanostructured Composites, Sungkyunkwan Advanced Institute of Nanotechnology, Sungkyunkwan University, Suwon 440-746, South Korea, and [‡]Energy Lab., Corporate R&D Center, Samsung SDI, Yongin 446-577, South Korea

ABSTRACT We propose a new material for high power and high density supercapacitors with excellent cycle stability. Graphite oxide (PSS—GO) intercalated with poly(sodium 4-styrensulfonate) showed high performance of electric double layer capacitance (EDLC) compared to that of the pristine graphite oxide. Specific capacitance of the PSS—GO reached 190 F/g, and the energy density was much improved to 38 Wh/kg with a power density of 61 W/kg. Cycle test showed that the specific capacitance decreased by only 12% after 14860 cycles, providing excellent cyclic stability. The high EDLC performance of PSS—GO composite was attributed to the wide interlayer distance and simple pore structures accommodating fast ion kinetics.

KEYWORDS: graphite oxide · supercapacitor · electric double layer capacitor · poly(sodium 4-styrensulfonate) · electrolyte ion kinetics

Energy storage devices, in particular electrochemical capacitors, are receiving a lot of attention recently for building up a green renewable energy environment. The electrochemical capacitors, also known as supercapacitors, have high power density and long cycle lifetime compared to batteries and have been used in such applications as memory back-up, emergency power supply, hybrid bus, and solar cell panels.[1−7] However, its low energy density has limited its use for numerous possible applications. Therefore, improvement of the energy density of supercapacitors is a prerequisite for developing green energy environment.

Graphite oxide (GO) and graphene supercapacitors have been investigated recently.[8−11] However, the specific capacitance and energy density are still low (below 10 Wh/kg) compared to other supercapacitors.[12−16] Interlayer distance in the case of graphite oxide shrinks during the charging/discharging process, which results in a reduction of the capacitance. The shrinkage also takes place during the thermal annealing at 100 °C required in the manufacture of supercapacitor electrodes.[11] Introduction of a simple thermally stable bridge between the interlayers of graphite oxide will make the interior layers available for ion storage/retrieval. This paper reports the enhanced performance of a GO supercapacitor with such a structure made by poly(sodium 4-styrensulfonate) (PSS) which has a high melting point (around 400 °C) and is water-soluble as well as nontoxic. The physical properties, thermal stability, and functional groups of the PSS-intercalated graphite oxide (PSS—GO) composites have been well investigated by our group.[17] However, the electrochemical properties of the composite are still missing. We herein show the electrochemical properties of PSS—GO composite which demonstrated high performance of electric double layer capacitance (EDLC) compared to that of the pristine graphite oxide. Specific capacitance of the composite reached 190 F/g, and energy density was much improved up to 38 W · h/kg with a power density of 61 W/kg. Cycle test of the cell showed excellent cyclic stability in which the specific capacitance decreased only by 12% after 14860 cycles.

The synthesis method of the PSS—GO composites has been reported earlier.[17] First, graphite oxide (GO) was synthesized by the modified Brodie's method.[18] The graphite oxide obtained (200 mg) was then dispersed in deionized water (250 mL) by a slow addition of 0.1 M NaOH aqueous solution until the pH was equal to 10. The solution was further sonicated for 1 h. The PSS

*Address correspondence to leeyoung@skku.edu.

Received for review December 9, 2009 and accepted January 18, 2010.

Published online January 25, 2010. 10.1021/nn901790f

aqueous solution was made from 2 g of PSS (Sigma-Aldrich, MW = 18000) and 200 mL of DI water. The mixture was sonicated for 10 min for better dissolution (pH = 4.9). The two solutions (GO and PSS) were then mixed and stirred for 12 h (pH = 8.0). Then, the PSS−GO composite was formed into a thin film (average thickness of 45 μm) on a filter (0.1 μm, Anodisc 47, Whatman) by a slow filtration for over a day. Graphite oxide thin film was also prepared as a reference as follows. The graphite oxide (2 g), polyvinylidene fluoride (PVDF, 4.17 g), and kitchen black (KB, 0.25 g) were mixed in *N*-methylpyrrolidone (NMP). The mixture was spread onto 15 μm thick aluminum foil with a micrometer adjustable film applicator, oven-dried at 110 °C for 6 h, and roll pressed into a film (thickness ≈ 137 μm).

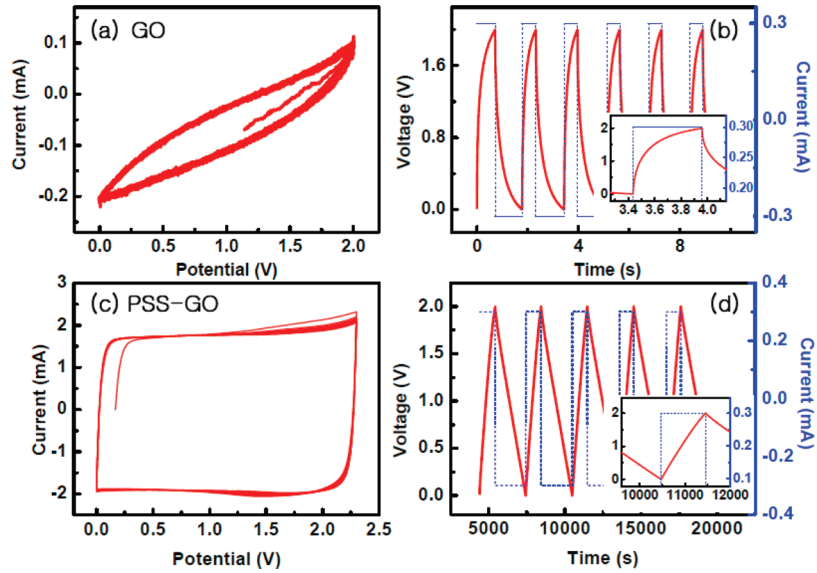

Figure 1. Cyclic voltammetry and galvanostatic charge/discharge curves of graphite oxide (a, b) and PSS−GO (c, d). The scan rate was 10 mV/s and cycles of 10 times in CV, and the current density of charge−discharge curves was 0.1 A/g with a discharge voltage of 2.0 V.

Thin films of the PSS−GO composite and GO were punched to make a round shape electrode for a 1.6 cm diameter coin cell (Wellcose, CR2016). The coin cell comprises two electrodes that are isolated from electrical contact by a porous separator. The separator and electrodes are impregnated with tetraethyl ammonium tetrafluoroborate ($TEABF_4$, 1.0 M) that was dissolved in propylene carbonate (PC). Electrochemical characteristics were examined using a multichannel potentiostat and galvanostat with an impedance spectroscopy (Bio-Logic Science Instruments, France). The cyclic voltammetry was collected at a scan rate of 10 mV/s. The gravimetric capacitance of the electrodes was calculated according to $C_g = i/(\nu m)$, where i is the current, ν is the scan rate or the linear slope of the discharging curve, and m is the mass of active electrode. Energy and power density (E, P) were calculated by the equations in which $E = {}^1/_2 C_{total} V^2$ and $P = 2E$/unit time, respectively, where C_{total} is the total capacitance of the cell.[19]

Cyclic voltammetry of graphite oxide (GO) in Figure 1a shows an elliptical curve, indicating a faradaic reaction at the interface of electrodes with electrolyte ions, which is a typical behavior of pseudocapacitors. The current increases slowly as the potential increases, implying that the electric conductivity of GO is too low to transfer charges quickly. Galvanostatic charge−discharge curve of GO in Figure 1b also supports the pseudocapacitive behavior because the charging/discharging curve is nonlinear in GO. The nonlinearity indicates contribution of pseudocapacitance due to the faradaic reaction. The IR drop in the discharging curve is also shown in the inset of Figure 1b. In the case of the PSS−GO composite, however, the cyclic voltammetry shows a big rectangular shape (Figure 1c), which is a typical behavior of electric double layer capacitor (EDLC). The current increased quickly as the potential increased and remained almost constant until the potential reached the maximum, and vice versa. The linear curve simply indicates of the PSS−GO composite support the EDLC capacitive behavior due to the nonfaradaic interaction (Figure 1d). No appreciable IR drop was observed, as evidenced by the inset. This is attributed to the improvement of conductivity of the electrode by the PSS intercalation. Gravimetric capacitance was calculated from the Galvanostatic charge/discharge curves. The specific capacitance of several GO samples ranged from 0.05 to 14 F/g. On the other hand, the capacitance was improved up to 190 F/g in the case of PSS−GO samples. Average equivalent series resistance (ESR) can be calculated from the ohmic drops in the discharge curves,[3] which was about 1400 and 3 ohm for the GO and PSS−GO samples, respectively. The ESR of the PSS−GO composite was lower by 3 orders of magnitudes than that of the pristine GO. The low resistance of the composite provides easy transport of charges, resulting in high power density. The enhanced conductance of the PSS−GO composite compared to that of GO was predicted in the previous study in which the conductance was derived from the dielectric constant measurement, and the PSS−GO composite showed higher conductance by 3 orders of magnitudes than that of GO sample.[17] This is consistent with the current ESR results.

The dependence of the gravimetric capacitance on the current density was presented in Figure 2a. The capacitance was 190 F/g at 0.1 A/g, and reduced and saturated to about 90 F/g until the current density was 30 A/g with a discharge voltage of 2.0 V. The corresponding energy density *versus* power density was plotted in Figure 2b, marked by red-filled squares. When the discharge voltage increased to 2.7 V, the energy density also increased up to 38 W · h/kg at a power density of

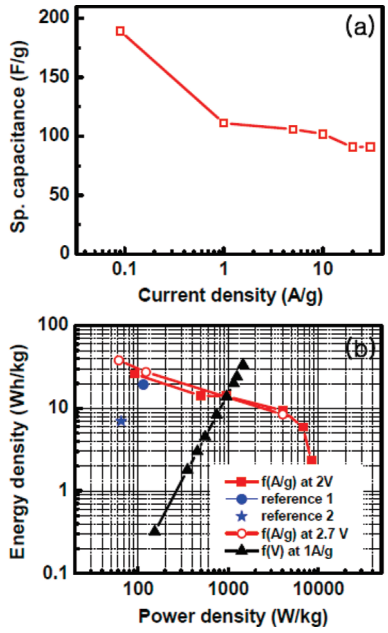

Figure 2. (a) Gravimetric capacitance as a function of the current density, resulting from the galvanostatic measurement. (b) Ragone plot of PSS−GO composites as a function of current density at 2 V (filled squares) and 2.7 V (open circles), discharge voltage at 1 A/g (filled triangles), and references (filled star and circle from the ref 21 and 22).

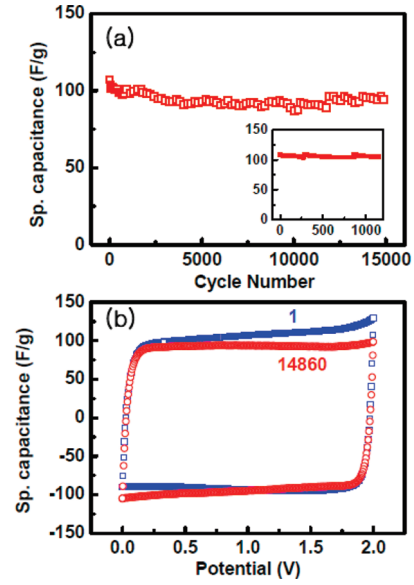

Figure 3. (a) Specific capacitance as a function of the cycle number. Inset shows the cycle test of different batched sample cell. (b) Cyclic voltammetry of the first and after 14860 cycles of PSS−GO sample (scan rate was 10 mV/s).

61 W/kg, marked by open circles in Figure 2b. The maximum energy density obtained was 38 W · h/kg, which is significantly improved compared to the previous reports,[7,8,12,20,21] marked by the filled circle and star in the Ragone plot (Figure 2b). The energy density also increased from 0.3 to 34 Wh/kg as the discharge voltage increased linearly from 0.4 V up to 3.0 V at a current density of 1 A/g, marked by filled triangles in Figure 2b. This indicates that the $TEABF_4$/PC electrolyte is reliable in the high voltage region for high energy density supercapacitor applications.

High electrochemical stability was found by the repeated galvanostatic charge/discharge cycling (2 V, 1 A/g) and cyclic voltammetry (2 V, 10 mV/s) from different batches of the PSS−GO cells as shown in Figure 3. The specific capacitance decreased very slowly until 14860 cycles and decreased by only 12% of the initial capacitance, indicating that the capacitor has an excellent cycle life. The inset shows the cycle test of another cell, indicating reproducible cyclic behavior. Figure 3b presents the cyclic voltammetry of the first and after 14860 cycles, and the rectangular shape, indicating that the EDLC contribution still remained after the long cycle test. The charging and discharging curves became flattened compared to the first cycle. This indicates that the contribution from faradaic reaction was completely removed after first few cycles. The nonfaradaic EDLC contribution then survives for a long cycle test without an appreciable degradation. In this sense, it is conjectured that the contribution from faradaic reaction is less than 12%.

The reason for higher capacitance and energy density of the PSS−GO composite can be seen in absorption/desorption measurement of charges at a constant potential ($V = 2$ V for absorption and $V = 0$ V for desorption) as shown in Figure 4a. The PSS−GO cell shows higher charge absorption/desorption (~current of 400 mA) compared to that of the GO cell (~current of 2 mA). Rectangular dashed box in Figure 4a was marked to see the charge absorption/desorption of the GO cell in detail. Figure 4b was the magnification of the dashed box, indicating very small current in GO is by absorption and desorption of ions. The integrated current during absorption (desorption) time indicates the total charges of absorption (desorption). The calculated average absorbed charges of GO and PSS−GO capacitor were 72 and 392 mC, respectively, resulting in 5.5 times higher charge absorption in the PSS−GO capacitor. As for the average desorbed charges, the GO has 43 mC and the PSS−GO capacitor has 328 mC, which is about 5 times higher than that of the pristine GO capacitor. The high absorption and desorption of charges in the PSS−GO capacitor is strongly coupled to the high capacitance and energy density, which is consistent with the CV and galvanostatic charge−discharge results.

To evaluate adsorption rate constants, the measure of how fast ions transport and adsorb into pores, the adsorption data were fitted to the first order kinetic equation; $Q_t = Q_e (1 - e^{-kt})$, where k is the adsorption rate constant, and Q_t and Q_e are the amount of charges adsorbed at time t and equilibrium, respectively. Figure 4 panels c and d show the curve fittings with the absorbed charges with times of GO and PSS−GO, respectively. Even though the fitting is poor, especially in the case of GO, the adsorption rate constant of 0.009 for GO

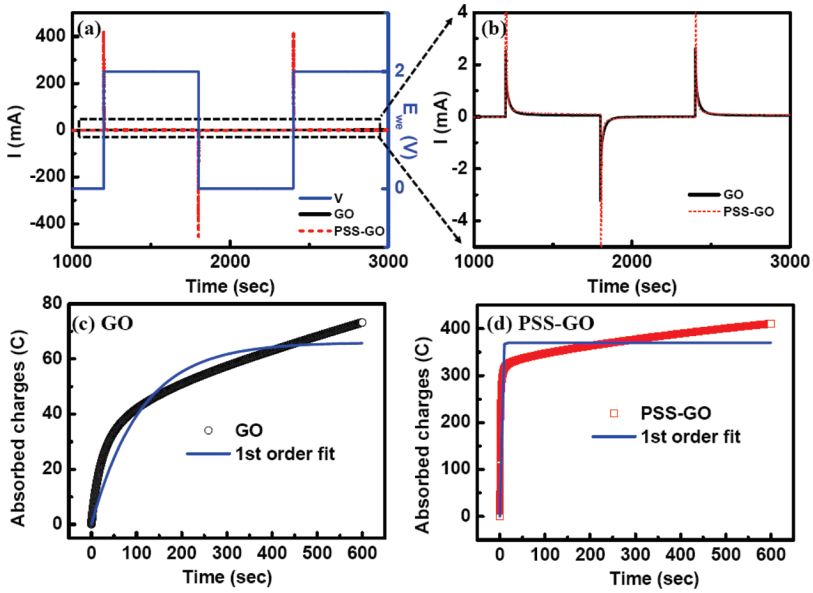

Figure 4. (a) Absorption and desorption of charges in GO and PSSGO cell under constant potential (2 V for absorption and 0 V for desorption). Rectangular dashed box near zero current was marked to see detail GO result. (b) Magnification of the dashed box for the GO result. Integrated absorbed charges of (c) GO and (d) PSS−GO cell were shown with the best curve fitting with the first order kinetic equation.

and 0.48 for PSS−GO from the first order kinetic equation gave qualitative comparison between GO and PSS−GO. The 50-fold increase in the rate constant can originate from several factors. One is the enhanced interlayer distance (of up to 8 Å) in the case of the PSS−GO. Another is a robust prohibition of redox reactive sites blocked by the PSS. Some redox groups such as epoxide and hydroxyl groups in the pristine GO are mostly covered by the PSS. Carboxylic groups that are present at the edge of GO[18,22−24] could also be blocked, which results in facilitating an easy transport of ions. As a consequence, not only the redox reaction is suppressed but also robust pore pathways become available thereby enhancing the ion kinetics.

The high EDLC capacitive behavior of the PSS−GO was also shown in Nyquist plots, an impedance behavior as a function of frequency. At lower frequency regime, the GO shows a slow diffusion resistance (Figure 5a), indicating the Faradaic reaction, which is the reason for the nonrectangular and nonlinear shapes of CV and galvanostatic charge/discharge cycles, while the PSS−GO shows very steep slope and only imaginary impedance in the same frequency regime, indicating excellent EDLC performance (Figure 5b). The ESR of GO and PSS−GO were obtained from the semicircles in insets, about 40 Ω for GO and 15 Ω for PSS−GO. However, ESR of 15 Ω is still large enough for PSS−GO showing poor power density characteristics. Additional studies are needed to decrease the ESR of PSS−GO and will be investigated in the near future.

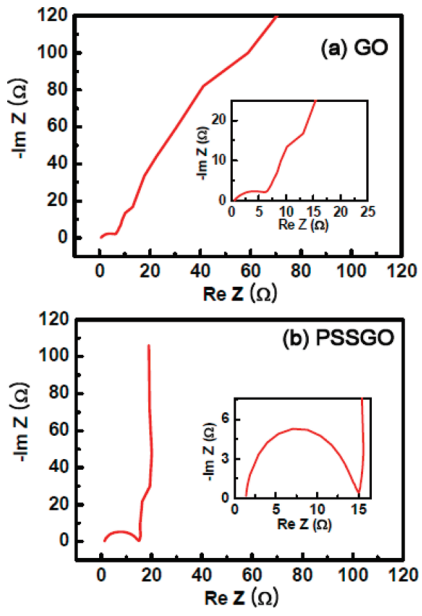

Figure 5. Nyquist plot of (a) GO and (b) PSS−GO in frequency regime from 10 mHz to 100 kHz. Insets show magnification of the impedance near zero and corresponding semicircle marked by dashed line.

It is worth noting that the surface area of GO and PSS−GO is very low (3.2 and 9.5 m^2/g for GO and PSS−GO) according to the BET measurement under N_2 gas. The nitrogen gas somehow could not enter the interlayers in both of GO and PSS−GO, but the electrolyte ions could propagate well, especially in the case of PSS−GO as shown in Figure 4. In addition, the surface area estimates from the BET measurement took account of only pores which were less than 100 nm. Larger pores could be contributing to the improved performance in charge storage. Detailed *in situ* change of interlayer distance, surface area, and chemical components in the electrolyte should be studied further.

In conclusion, we have investigated the electrochemical properties of the PSS−GO capacitors. The cyclic voltammetry and galvanostatic charge−discharge cycles of the composites showed excellent EDLC performance and stable specific capacitance with high current density. Energy density was improved up to 38 W · h/kg with a power density of 61 W/kg, and the specific capacitance decreased by only 12% after 14860 cycles, providing excellent cyclic stability. The superior EDLC performance of the PSS−GO opens new possible material as a strong candidate for supercapacitor of high energy density.

Acknowledgment. This work was supported by the STAR faculty project in the Ministry of Education, in part by KOSEF through the CNNC at Sungkyunkwan University, and in part by the National Research Foundation of Korea funded by the Ministry of Education, Science and Technology (2009-0087138). This research was also supported by WCU (World Class University) program through the National Research Foundation of Korea funded by the Ministry of Education, Science and Technology (R31-2008-000-10029-0).

REFERENCES AND NOTES

1. Sarico, A. S.; Bruce, P.; Scrosati, B.; Schalkwijk, W. V. Nanostructured Materials for Advanced Energy Conversion and Storage Devices. *Nat. Mater.* **2005**, *4*, 366–377.
2. Simon, P.; Gogotsi, Y. Materials for Electrochemical Capacitors. *Nat. Mater.* **2008**, *7*, 845–854.
3. Conway, B. E. *Electrochemical Supercapacitors*; Kluwer Academic and Plenum: New York, 1999; pp 12−156.
4. Service, R. New Supercapacitor Promises to Pack More Electrical Punch. *Science* **2006**, *313*, 902.
5. Sriparagorn, A.; Limwuthigraijirat, N. Experimental Assessment of Fuel Cell/Supercapacitor Hybrid System for Scooters. *Int. J. Hydro. Energy* **2009**, *34*, 6036–6044.
6. Bernard, J.; Delprat, S.; Büchi, F.; Guerra, T. Fuel-Cell Hybrid Powertrain: Toward Minimization of Hydrogen Consumption. *IEEE Trans. Vehicle Technol.* **2009**, *58*, 3168–3176.
7. Raymundo-Piñero, E.; Cadek, M.; Béguin, F. Tuning Carbon Materials for Supercapacitors y Direct Pyrolysis of Seaweeds. *Adv. Func. Mater.* **2009**, *19*, 1032–1039.
8. Stoller, M. D.; Park, S.; Zhu, Y.; An, J.; Ruoff, R. S. Graphene-Based Ultracapacitors. *Nano Lett.* **2008**, *8*, 3498–3502.
9. Ka, B. H.; Oh, S. M. Electrochemical Activation of Expanded Graphite Electrode For Electrochemical Capacitor. *J. Electrochem. Soc.* **2008**, *155*, A685–A692.
10. Wang, D.; Li, F.; Wu, Z.; Ren, W.; Cheng, H. M. Electrochemical Interfacial Capacitance in Multilayer Graphene Sheets: Dependence on Number of Stacking Layers. *Electrochem. Commun.* **2009**, *11*, 1729–1732.
11. Kim, I. J.; Yang, S.; Jeon, M. J.; Moon, S. I.; Kim, H. So.; Lee, Y. P.; an, K. H.; Lee, Y. H. Structures and Electrochemical Performances of Pyrolized Carbons from Graphite Oxides for Electric Double-Layer Capacitor. *J. Power Sources* **2007**, *173*, 621–625.
12. Kaempgen, M.; Chan, C. K.; Ma, J.; Chi, Y.; Gruner, G. Printable Thin Film Supercapacitors Using Single-Walled Carbon Nanotubes. *Nano Lett.* **2009**, *9*, 1872–1876.
13. Zhang, H.; Cao, G.; Wang, Z.; Yang, Y.; Shi, Z.; Gu, Z. Growth of Manganese Oxide Nanoflowers on Vertically-Aligned Carbon Nanotube Arrays for High-Rate Electrochemical Capacitive Energy Storage. *Nano Lett.* **2008**, *8*, 2664–2668.
14. Cao, L.; Xu, F.; Liang, Y.; Li, H. L. Preparation of the Novel Nanocomposite $Co(OH)_2$/Ultrastable Y Zeolite and Its Application as a Supercapacitor with High Energy Density. *Adv. Mater.* **2004**, *16*, 1853–1857.
15. Kim, J. Y.; Kim, K. H.; Kim, K. B. Fabrication and Electrochemical Properties of Carbon Nanotube/Polypyrrole Composite Film Electrodes with Controlled Pore Size. *J. Power Sources* **2008**, *176*, 396–402.
16. An, K. H.; Kim, W. S.; Park, Y. S.; Moon, J. M.; Bae, D. J.; Lim, S. C.; Lee, Y. S.; Lee, Y. H. Electrochemical Properties of High-Power Supercapacitors Using Single-Walled Carbon Nanotube Electrodes. *Adv. Funct. Mater.* **2001**, *11*, 387–392.
17. Jeong, H. K.; Jin, M. H.; An, K. H.; Lee, Y. H. Structural Stability and Variable Dielectric Constant in Poly(sodium 4-styrensulfonate) Intercalated Graphite Oxide. *J. Phys. Chem. C* **2009**, *113*, 13060–13064.
18. Jeong, H. K.; Lee, Y. P.; Lahaye, R.; Park, M. H.; An, K. H.; Kim, I. J.; Wnag, C. W.; Park, C. Y.; Ruoff, R. S.; Lee, Y. H. Evidence of Graphitic AB Stacking Order of Graphite Oxides. *J. Am. Chem. Soc.* **2008**, *130*, 1362–1366.
19. Frackowiak, E. Carbon Materials for Supercapacitor Application. *Phys. Chem. Chem. Phys.* **2007**, *9*, 1774–1785.
20. Raymundo-Piñero, E.; Leroux, F.; Béguin, F. A High-Performance Carbon for Supercapacitors Obtained by Carbonization of a Seaweed Biopolymer. *Adv. Mater.* **2006**, *18*, 1877–1882.
21. Ra, E. J.; Raymundo-Piñero, E.; Lee, Y. H.; Béguin, F. High Power Supercapacitors Using Polyacrylonitrile-Based Carbon Nanofiber Paper. *Carbon* **2009**, *47*, 2984–2992.
22. Jeong, H. K.; Noh, H. J.; Kim, J. Y.; Jin, M. H.; Park, C. Y.; Lee, Y. H. X-ray Absorption Spectroscopy of Graphite Oxide. *Europhys. Lett.* **2008**, *67004*, 1–5.
23. Jeong, H. K.; Calakerol, L.; Jin, M. H.; Glans, P.; Smith, K. E.; Lee, Y. H. Unoccupied Electronic States in Graphite Oxides. *Chem. Phys. Lett.* **2008**, 499–502.
24. Jeong, H. K.; Noh, H. J.; Kim, J. Y.; Calakerol, L.; Glans, P.; Jin, M. H.; Smith, K. E.; Lee, Y. H. Comment on Near-Edge X-ray Absorption Fine-Structure Investigation of Graphene. *Phys. Rev. Lett.* **2008**, *102*, 099701−099701.